Shock-induced arrhythmogenesis in the human heart: a simulation study

Miguel O. Bernabeu[1,2], Mikael Wallman[3], Blanca Rodriguez[3]

[1]*Centre for Computational Science, University College London, UK*
[2] *CoMPLEX, University College London, UK*
[3] *Department of Computer Science, University of Oxford, UK*

Correspondence: miguel.bernabeu@ucl.ac.uk; CoMPLEX, Physics Building, Gower Street, London, WC1E 6BT, UK

Introduction

Electrical defibrillation through the application of electric shocks to the heart is an effective therapy against ventricular fibrillation. However, factors underlying the success or failure of defibrillation shocks remain unclear. Over the past years, defibrillation mechanisms have been extensively investigated on small animal models such as the rabbit. Nevertheless, authors (see, *e.g.* [1,2]) often acknowledge that extrapolation of their results to the human has to be made with caution due to differences in size, anatomy, and electrophysiology. Of particular relevance are the increase in wall thickness and the decrease of the proportion of tissue under the effects of tissue-bath interactions.

An electrical shock can induce ventricular fibrillation when applied within the period of time known as vulnerable window (VW) following the beginning of a cardiac cycle. Furthermore, arrhythmias can only be induced by shock strengths between a lower and an upper limit of vulnerability (LLV and ULV). A shock applied within the VW and with strength between LLV and ULV is said to be within the vulnerability area (VA). The mechanisms by which defibrillation shocks re-initiate VF are strongly linked to the mechanisms by which a shock induces VF if applied within the VA following pacing. It is therefore of critical importance for the correct treatment of arrhythmias to be able to characterise the VA.

The purpose of the current work is therefore two-fold: i) to develop a human model of cardiac defibrillation with patient-specific anatomy including fibre orientation and accurate transmembrane kinetics, and ii) to perform the first simulation study of shock-induced arrhythmogenesis in the human heart. The objective of this study is to understand how geometrical differences between human and rabbit hearts affect shock-induced electrical activity. We hypothesize that differences in wall thickness have an impact in the importance of tissue-bath interaction in shock-end polarisation and post-shock behaviour.

Methods

Computational model

In this work we use a patient-specific anatomical model including representation of both ventricles of a human heart. The model was generated from a ventricular surface definition obtained from computed tomography (CT) images as described in [3]. Data was originally provided by the CISTIB group of the Pompeu Fabra University, Spain. Since information regarding fibre orientation could not be recovered from the original images, we used a generation algorithm based on the Streeter model previously presented in [4]. Transmembrane kinetics are described with the Ten Tusscher 2006 ionic model [5]. The model included representation of the blood in the ventricular cavities and the perfusing bath. Chaste's bidomain solver [6] was used to simulate electrical activity across tissue and bath. The simulations were run in HECToR phase2a.

Protocol for determining vulnerability grids

The protocol used for determining the vulnerability grid was taken from similar studies in the rabbit heart [7,8]. The human ventricular model was first paced at the apex by means of an intracellular volumetric stimulus applied to all the cells below the z = 1.4cm plane. Squared monophasic shocks of

variable strength and 8ms duration were delivered at varying coupling intervals (CI) via two external plate electrodes located at the boundaries of the bath on the sagittal plane. The electrode closer to the right ventricle (RV) was the cathode and the electrode closer to the left ventricle (LV) was the anode

The criteria for considering a reentry as sustained were also taken from the literature [7]. In brief, the arrhythmia was considered non-sustained if it consisted of one or two extra beats following the shock. However, if a third reentry was observed the arrhythmia was considered sustained. The vulnerability window was considered to be the range of CI for which sustained arrhythmia was induced.

Results

Vulnerability grid

The following table presents the vulnerability grid of the ventricular defibrillation model developed. The symbols in the table represent: i) EB, an extra beat of non-reentrant nature induced by the shock, ii) NS, non-sustained arrhythmia according to the criteria described in the Methods subsection, and iii) F8, figure-of-eight reentry.

	290ms	305ms	320ms	335ms	350ms	365ms	390ms
$26 A/cm^2$	EB	NS	NS	NS	NS	NS	EB
$31 A/cm^2$	EB	NS	NS	NS	NS	NS	EB
$36 A/cm^2$	EB	F8	F8	F8	F8	F8	EB
$41 A/cm^2$	EB	F8	F8	F8	F8	F8	EB

The vulnerability window of the model spans a range of CI between 297.5 ± 7.5 ms and 372.5 ± 7.5 ms. The lower limit of vulnerability is 33.5 ± 2.5 A/cm^2. The upper limit of vulnerability could not be determined with the range of shocks strengths considered in this study.

Mechanisms leading to reentrant circuits

In agreement with previous studies [8] in rabbit, post-shock transmembrane potential distribution displays the well-known virtual electrode polarisation (VEP) pattern. On the epicardium, two areas of opposite polarisation can be observed: RV epicardium is depolarised while LV epicardium is repolarised. This corresponds to the opposite polarity of the closest electrode. Sharp gradients appear at the interface between both areas with the location determined by the shape of the ventricles. In all our simulations, transmural response to the shock is much more complex than what was observed in the epicardium. At shock-end, the LV wall and the septum exhibit large areas of repolarised tissue with islands of excitation. The isolated areas of depolarised tissue are a result of the use of the bidomain model with anisotropic conductivity ratios and rotating fibres in a constant electrical field [Trayanova et al., 2006]. In contrast, the RV wall is mostly depolarised at shock-end.

Figure 1 shows the outcome of a shock of strength $41 A/cm^2$ applied at CI of 335 ms. In this case, three rotors are induced in the anterior LV wall, posterior LV wall and the septum, respectively. The excitable gap in the RV quickly closes following shock-end. At t=20ms, a depolarisation front initiated

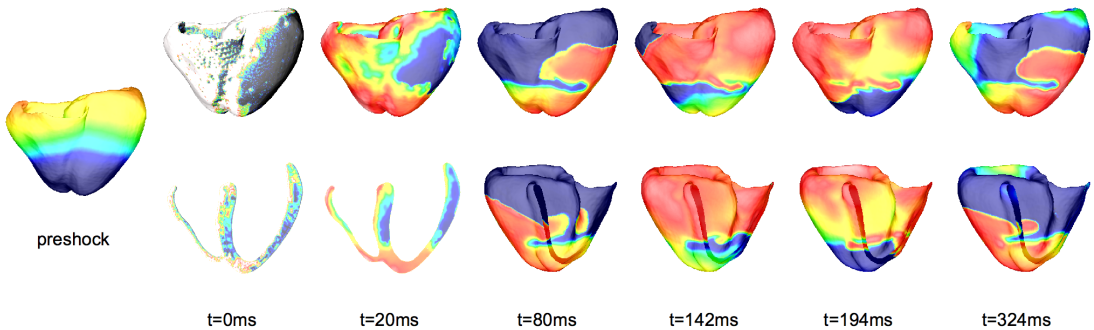

Figure 1: Figure-of-eight reentry with rotors in the anterior LV wall, posterior LV wall and septum. Shock strength 41A/cm2, CI=335ms.

at the apex finds its way up the LV wall. In the following 60 ms, the original wavefront becomes three reentrant waves anchored in the anterior LV wall, the posterior LV wall and the septum. Panels t=142 and t=194ms show how the interaction of the septal reentry and the other two is complex and could be easily mistaken for ectopical activation. At t=194ms the apical reentry terminates, however at t=324ms when the two main reentries start their second cycle the septal reentry is restarted again.

Conclusion

In this work, we developed a bidomain model of human shock-induced arrhythmogenesis including patient specific geometry, fibre orientation and representation of the blood in the ventricular cavities and the perfusing bath. The results show that sustained shock-induced arrhythmias occur for CI between 297.5± 7.5 ms and 372.5 ± 7.5 ms for an APD90 of 306ms and an average conduction velocity of 65cm/s. Shock-induced arrhythmias in the human model consist of figure-of-eight reentry with one rotor in the anterior and one rotor in the posterior of the ventricles. In some cases, a reentry is also established in the septum due to the large shock-induced excitable gap.

In previous studies in rabbit, the vulnerability windows included CI in the range [70,130], significantly shorter than in this study in human. This is due to differences in APD (96ms in rabbit vs 250ms in human). The study also shows that differences in size of the ventricular walls affect VEP and postshock behaviour. Previous studies in rabbit showed how the post shock excitable gap in the RV and septum disappears due to break excitation in areas with large gradients. In this study, we saw how this is still the case in the RV free wall but not in the septum. In our study, shock-induced arrhythmias in the human ventricles consist of figure-of-eight reentry, which is also the most commont type of reentry in studies of shock-induced arrhythmogenesis in rabbit.

Acknowledgements

This work was supported by the EC Framework 7 grants preDiCT (DGINFSO- 224381) and euHeart (BLROQL0). BR also holds a UK Medical Research Council Career Development Award. The authors would like to acknowledge the Chaste development team and the use of HECToR, UK's national high-performance computing service.

References

1. Maharaj, T., Blake, R., Trayanova, N., Gavaghan, D., and Rodriguez, B. (2008). The role of transmural ventricular heterogeneities in cardiac vulnerability to electric shocks. Progress in Biophysics and Molecular Biology, 96(1-3):321 – 338.
2. Rodríguez, B., Tice, B. M., Eason, J. C., Aguel, F., and Trayanova, N. (2004). Cardiac vulnerability to electric shocks during phase 1a of acute global ischemia. Heart Rhythm, 1(6):695 – 703.
3. Bernabeu, M. O., Wallman, M., and Rodriguez, B. (2010b). Shock-induced arrhythmoge- nesis in the human heart: A computational modelling study. In Engineering in Medicine and Biology Society (EMBC), 2010 Annual International Conference of the IEEE, pages 760–763.
4. Bernabeu, M. O., Bishop, M. J., Pitt-Francis, J., Gavaghan, D., Grau, V., and Rodriguez, B. (2008). High performance computer simulations for the study of biological function in 3D heart models incorporating fibre orientation and realistic geometry at para-cellular resolution. In Computers in Cardiology, 2008, pages 721–724.
5. ten Tusscher, K. H. W. J. and Panfilov, A. V. (2006). Alternans and spiral breakup in a human ventricular tissue model. American Journal of Physiology - Heart and Circulatory Physiology, 291(3):H1088–H1100.
6. Pitt-Francis, J., Pathmanathan, P., Bernabeu, M. O., Bordas, R., Cooper, J., Fletcher, A. G., Mirams, G. R., Murray, P., Osborne, J. M., Walter, A., Chapman, S. J., Garny, A., van Leeuwen, I. M., Maini, P. K., Rodríguez, B., Waters, S. L., Whiteley, J. P., Byrne, H. M., and Gavaghan, D. J. (2009). Chaste: A test-driven approach to software development for biological modelling. Computer Physics Communications, 180(12):2452– 2471.
7. Rodríguez, B., Li, L., Eason, J., Efimov, I., and Trayanova, N. (2005). Differences between left and right ventricular chamber geometry affect cardiac vulnerability to electric shocks. Circ Res, 97(2):168–75.
8. Rodríguez, B. and Trayanova, N. (2003). Upper limit of vulnerability in a defibrillation model of the rabbit ventricles. Journal of Electrocardiology, 36(Supplement 1):51 – 56.